

**Analysis of the binary
neutron star merger
GW170817 using
numerical-relativity
calibrated waveforms**

in prep.

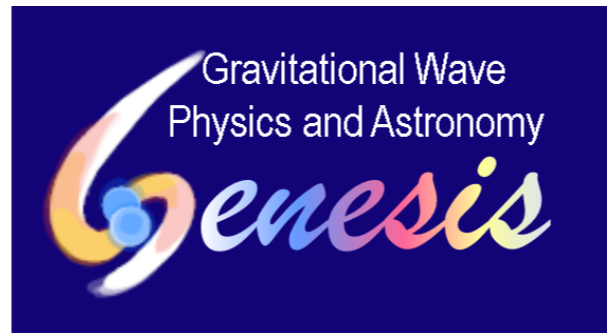
credit: NASA/Goddard Space Flight Center

Tatsuya Narikawa (Kyoto U. TAP)

Nami Uchikata, Kyohei Kawaguchi, Koutarou Kyutoku, Kenta Kiuchi,
Masaru Shibata, Hideyuki Tagoshi

"Multi-Messenger Astrophysics in the GW Era," 10/3, 2019, YITP

Gravitational Wave Physics and Astronomy: Genesis



Synergy between data analysis and theory researches

A: BH binaries

A-01

Testing gravity

A-02

Gravity and
Cosmology

A-03

BH binary
formation

B: NS binaries

B-01

Internal structure
of NS

B-02

Gamma-ray
burst and BH

B-03

r -process
elements

C: Supernovae

C-01

SN explosion
mechanism

C-02

SN explosion
mechanism via
 ν observation

Physics and astronomy motivated by GW observations

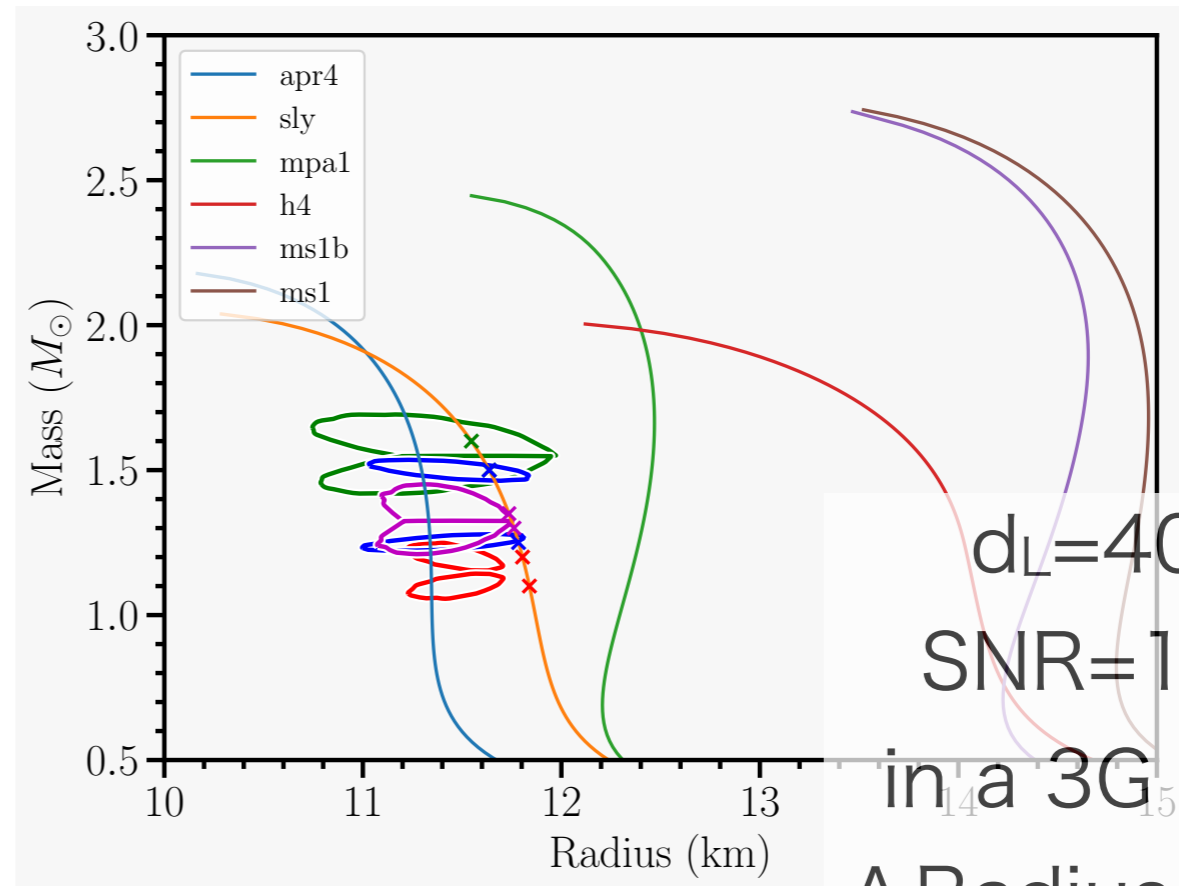
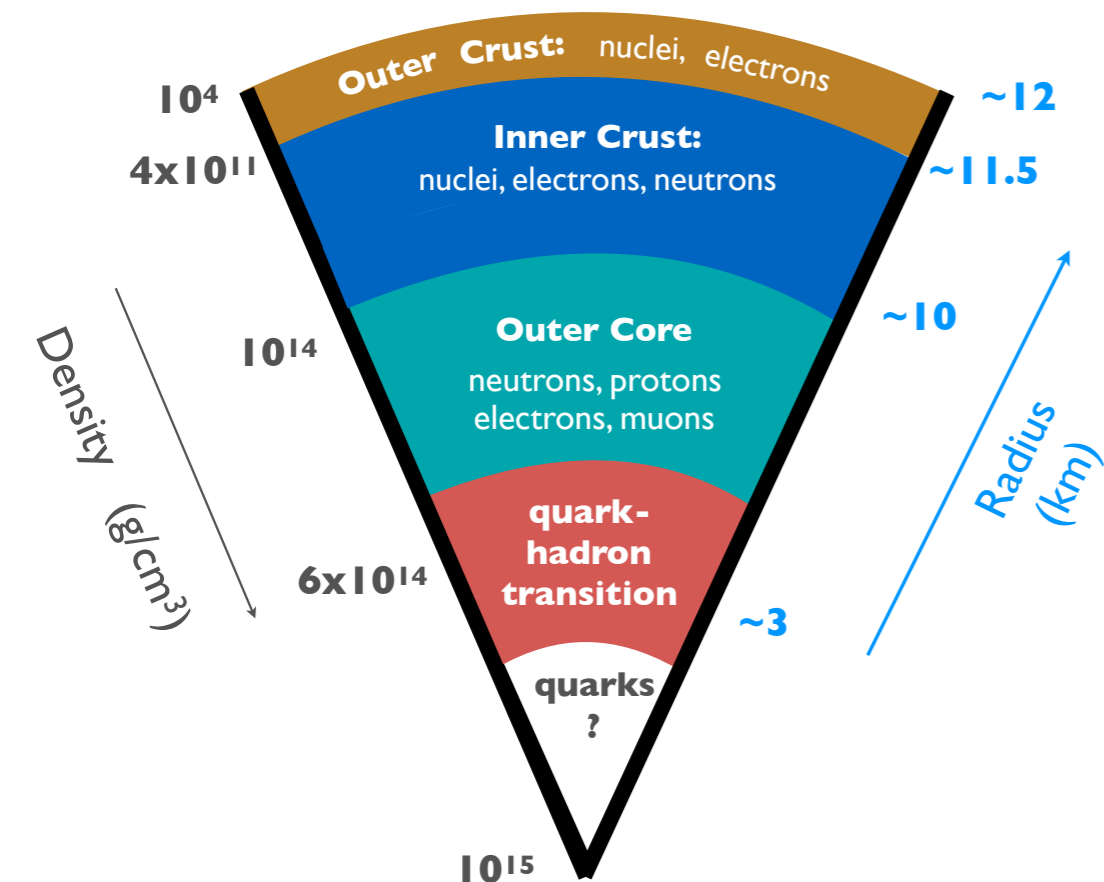
Fundamental physics

Structure of bulk matter at supranuclear density

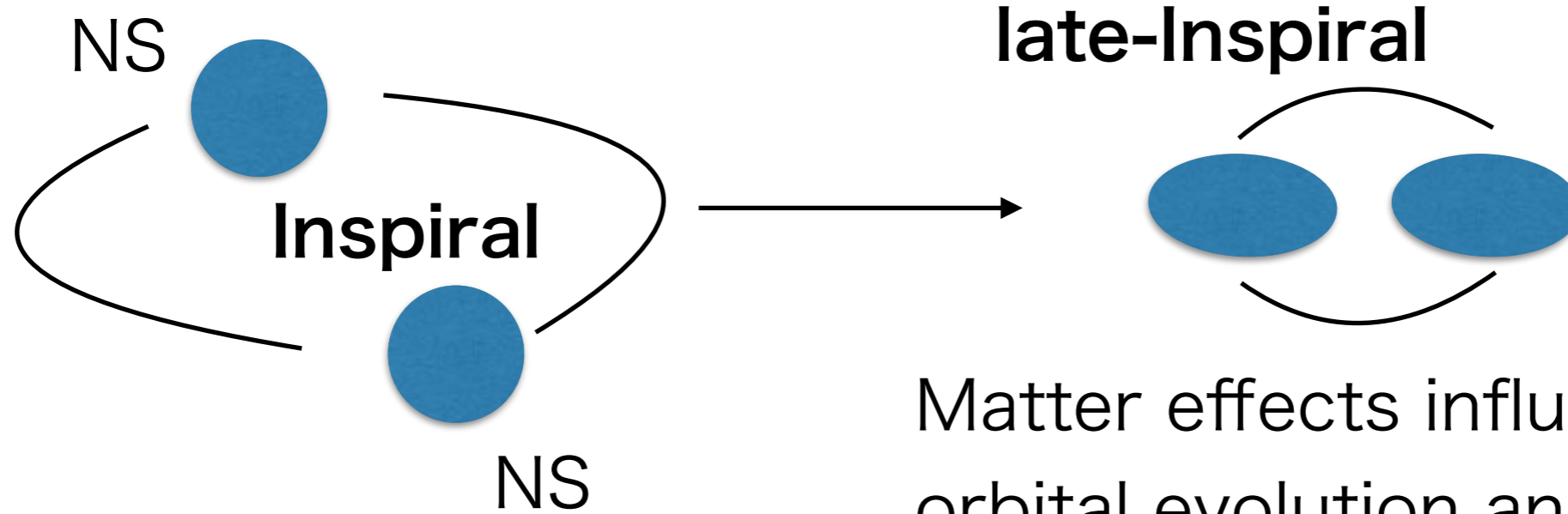
2. Extreme Matter, Extreme Environs

SCIENCE TARGET

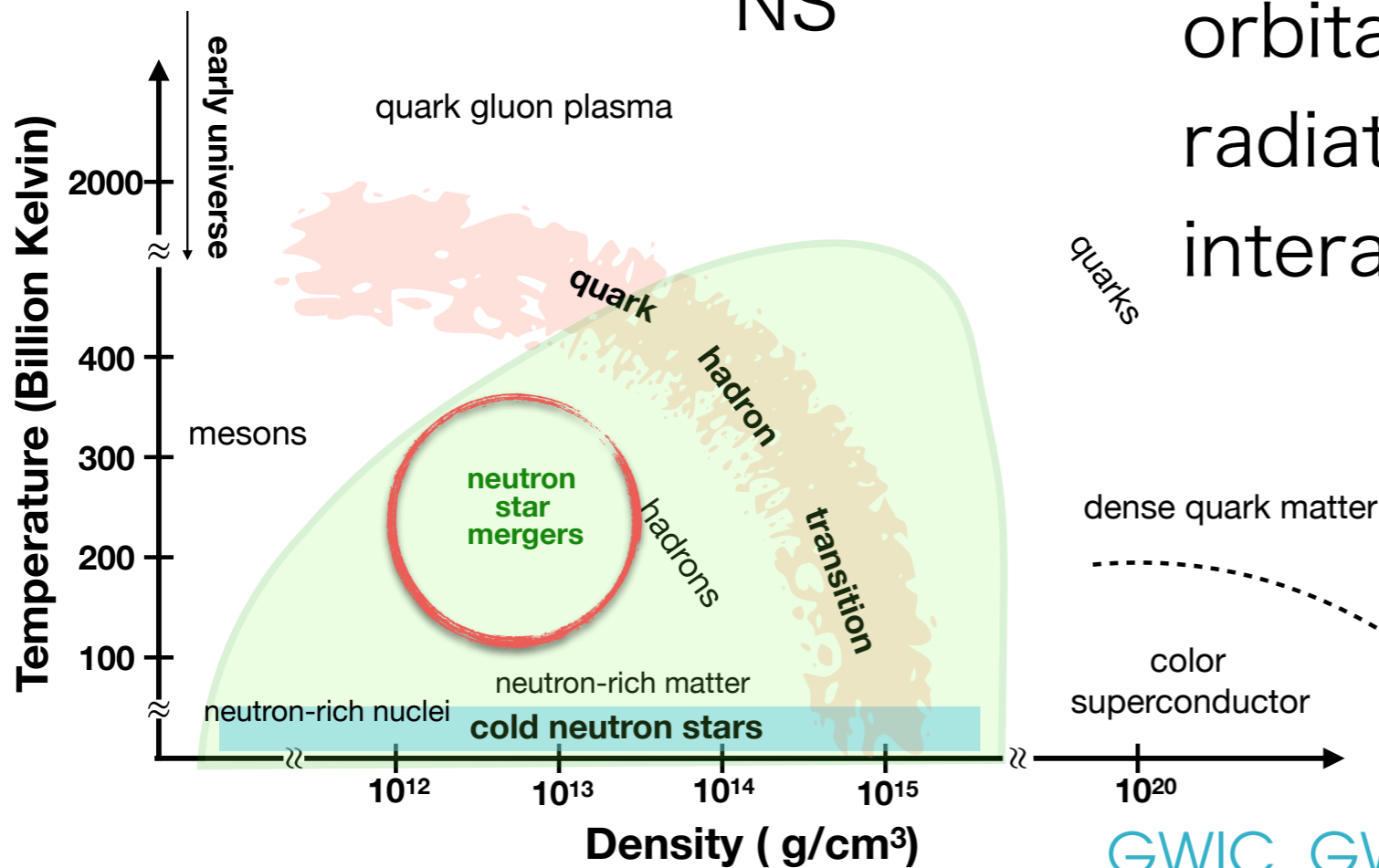
Determine the properties of the hottest and densest matter in the Universe



Binary-neutron-star (BNS) merger



Matter effects influence the orbital evolution and gravitational radiation through the tidal interaction between the NSs.

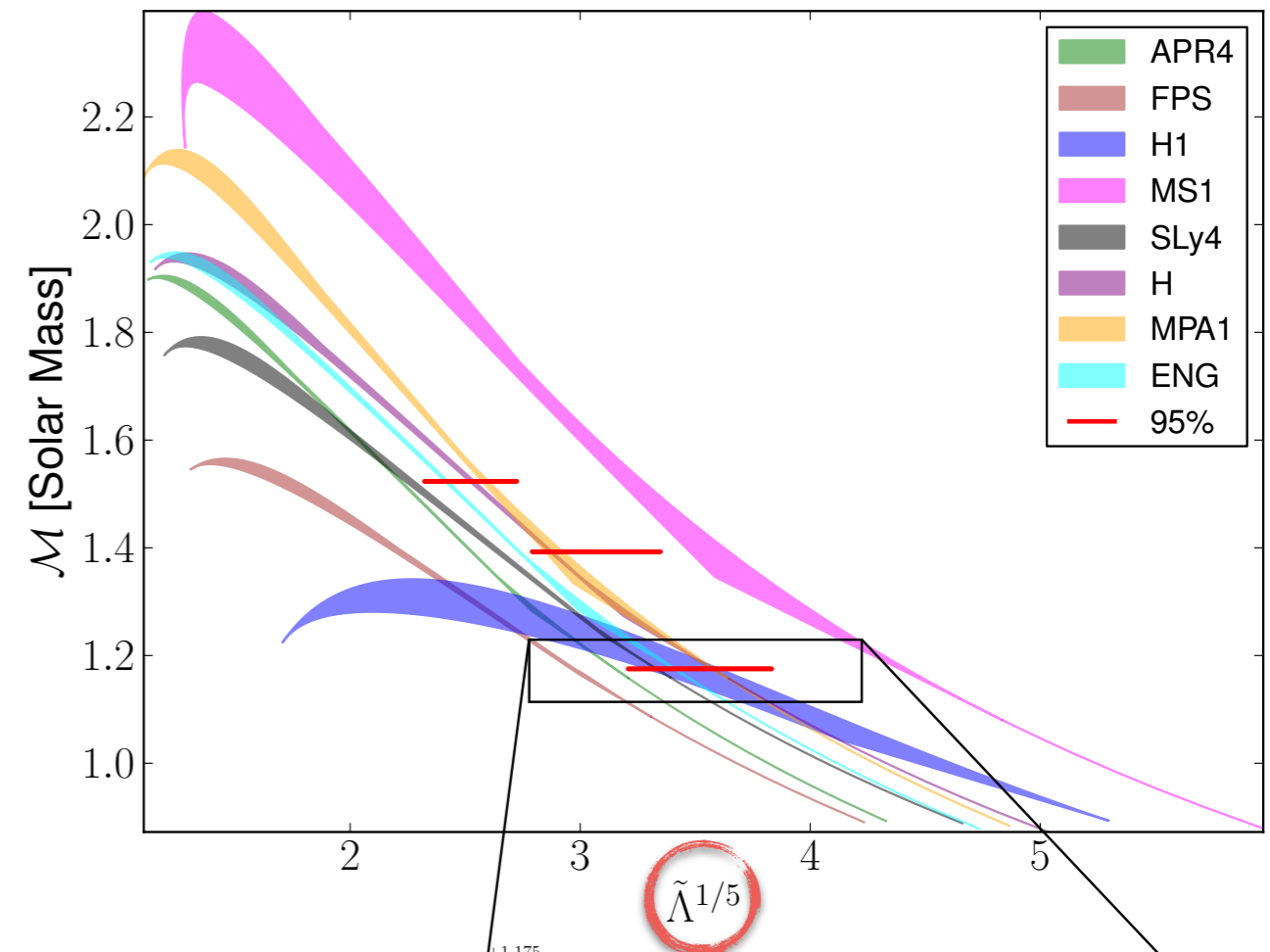
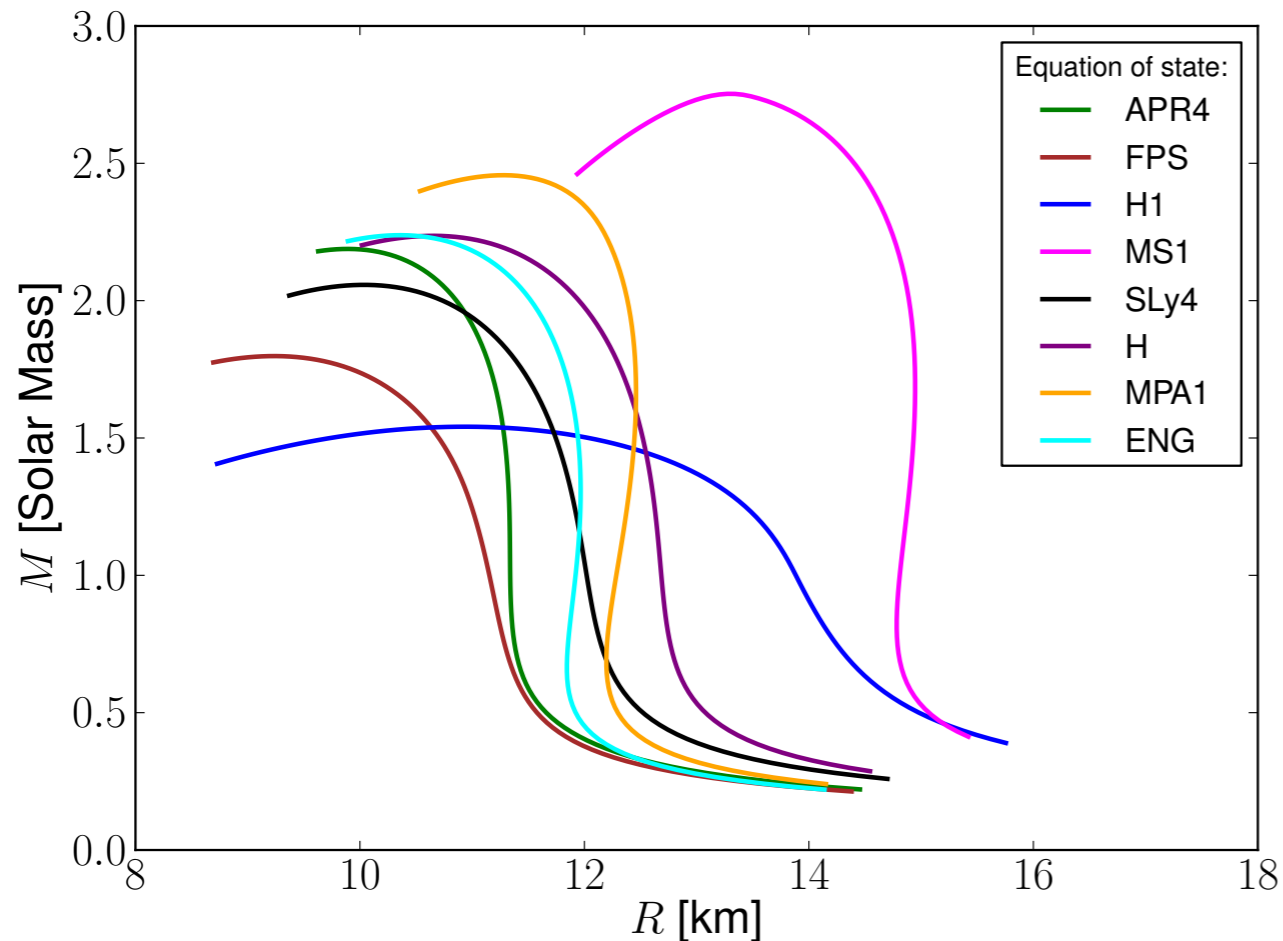


GWIC, GWIC-3G, GWIC-3G-SCT-Consortium

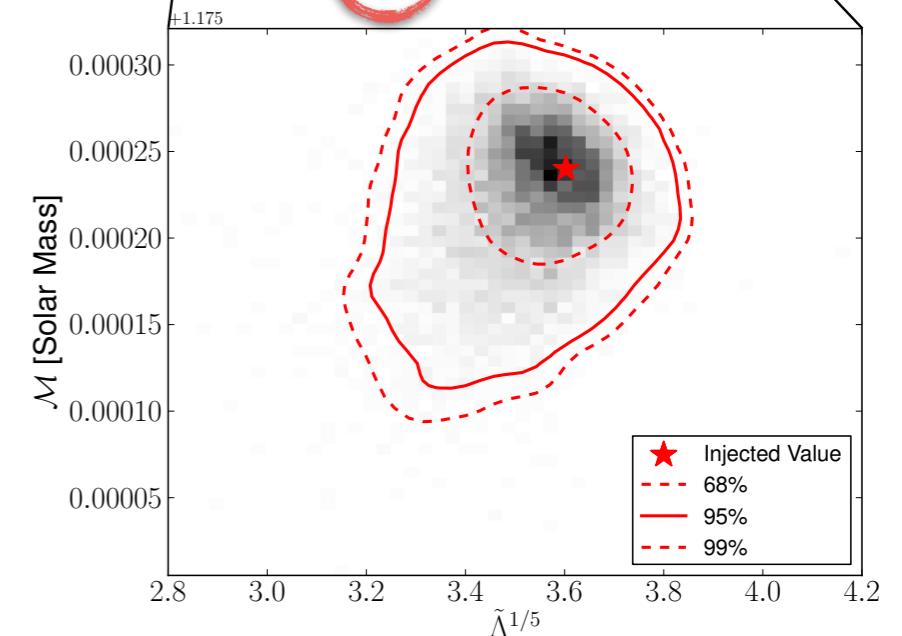
BNS mergers are valuable laboratories for nuclear astrophysics.

• Can GWs help constrain the NS EOS?

- To visualize how a GW detection might constrain the NS EOS, we plot a 2D PDF from a single source on mass-radius-*like* curves



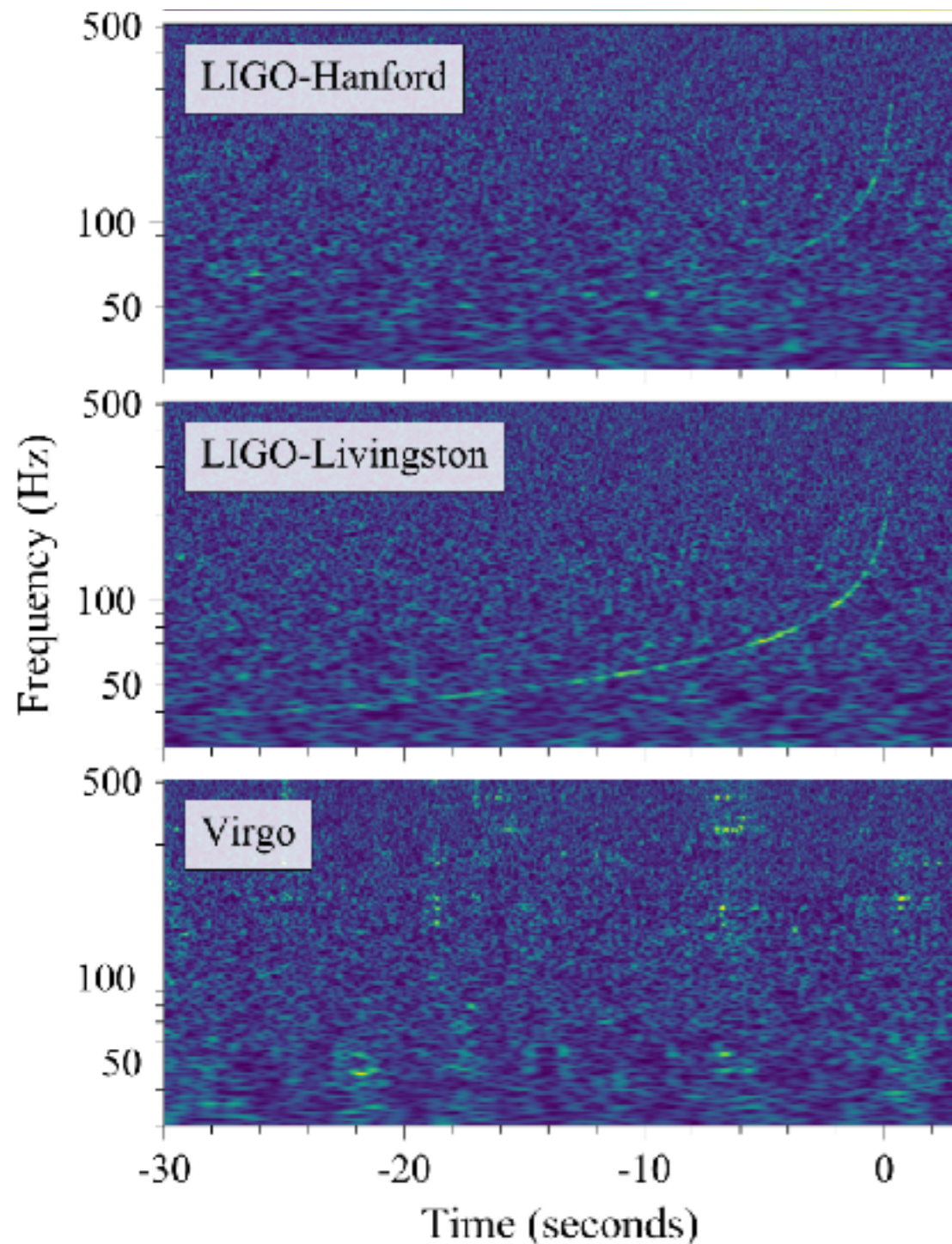
- We find that a single, loud (Network SNR 32.4) BNS GW detection can rule out several NS EOS families
- Multiple detections will highly constrain the NS EOS



Discovery of GW170817

[LVC, 2017]

Spectrograms

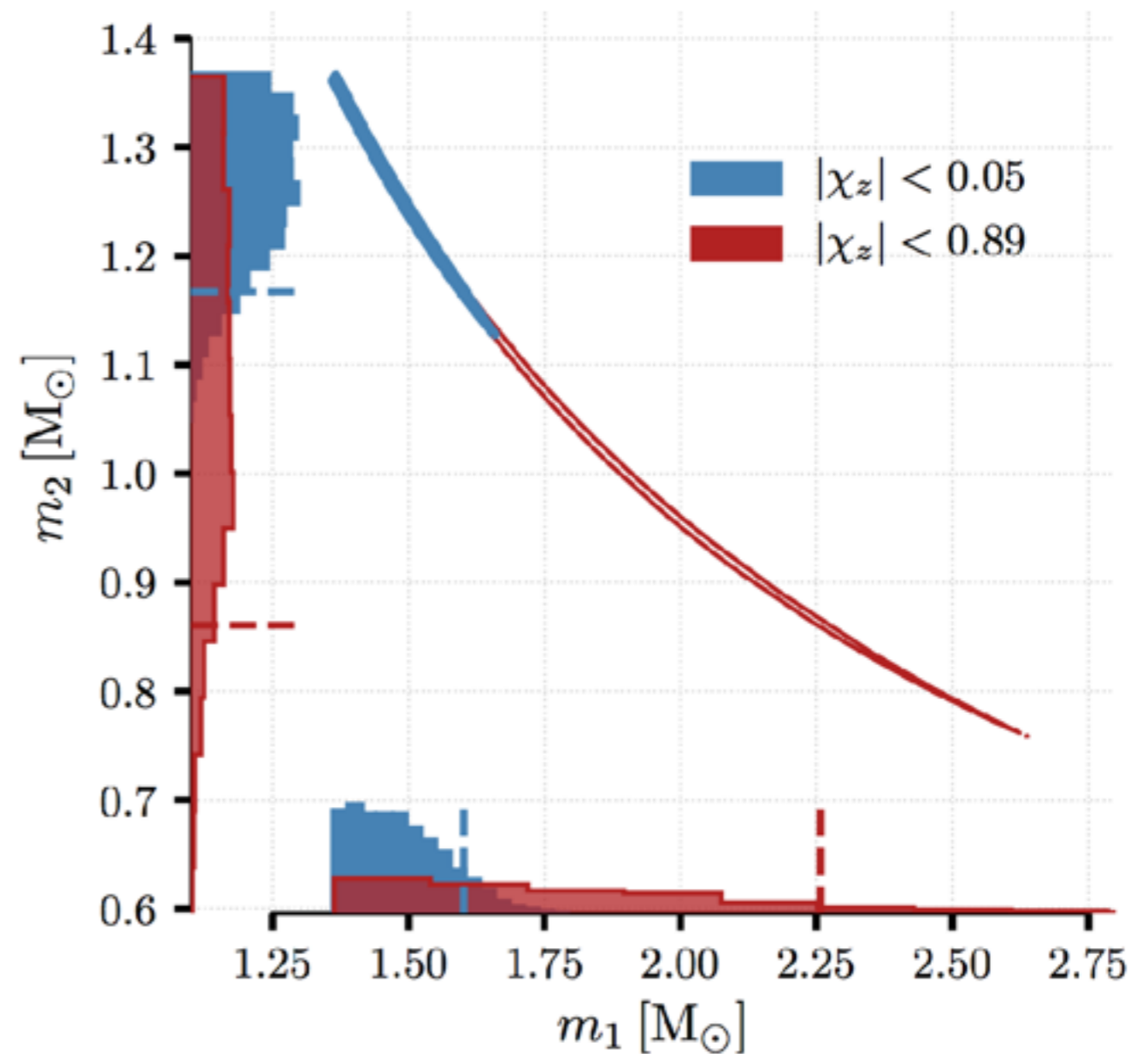


SNR

32.4 (Network)

18.8 (H), 26.4(L), 2.0 (V)

Estimates of the two components of the binary



GW170817 enabled us to measure the tidal deformability for the first time

[LVC, 2017]

Λ constrains the nuclear EOS of NS matter.

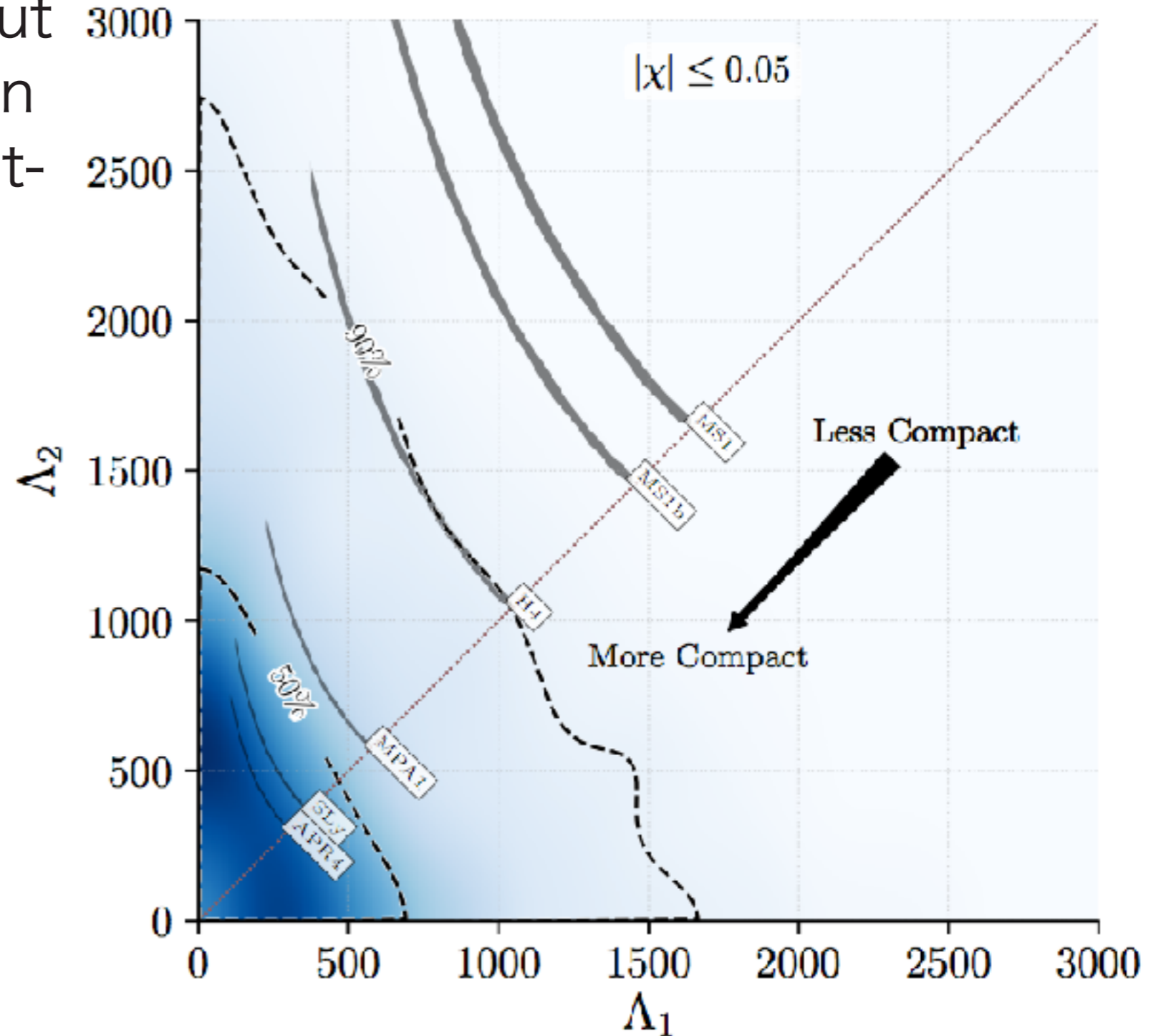
LIGO-Virgo Collaboration put conservative upper limits on tidal deformability with post-Newtonian waveform

(restricted TF2

with 5+1PNTidal).

symmetric contribution of tidal deformability

$$\tilde{\Lambda} \leq 900$$

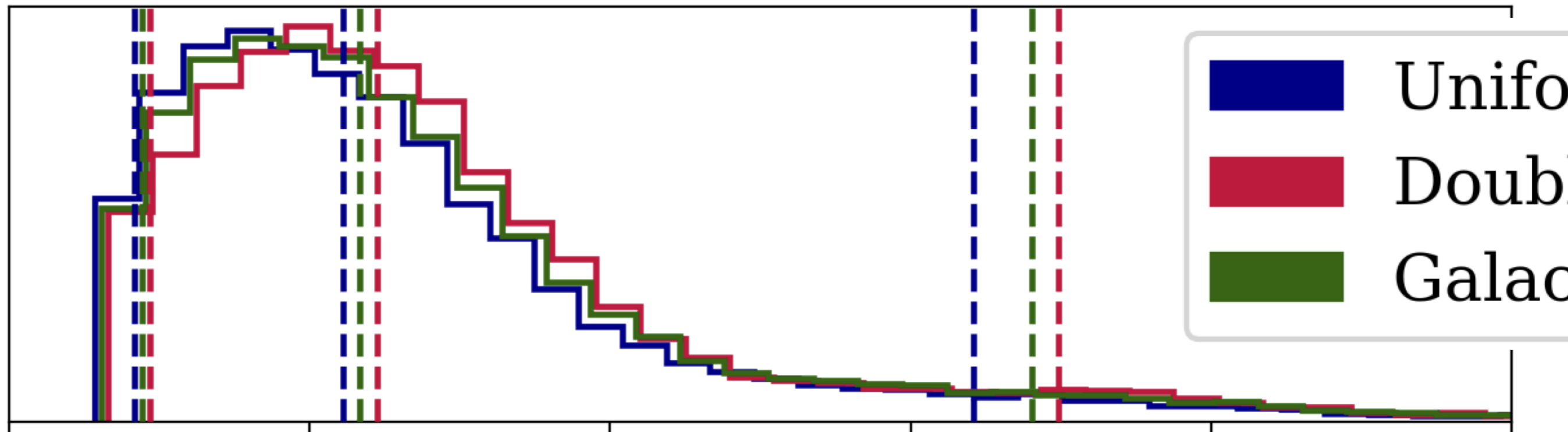


Independent analysis of GW170817

with restricted TF2 with 5+1PN Tidal

[De, et al., 2018]

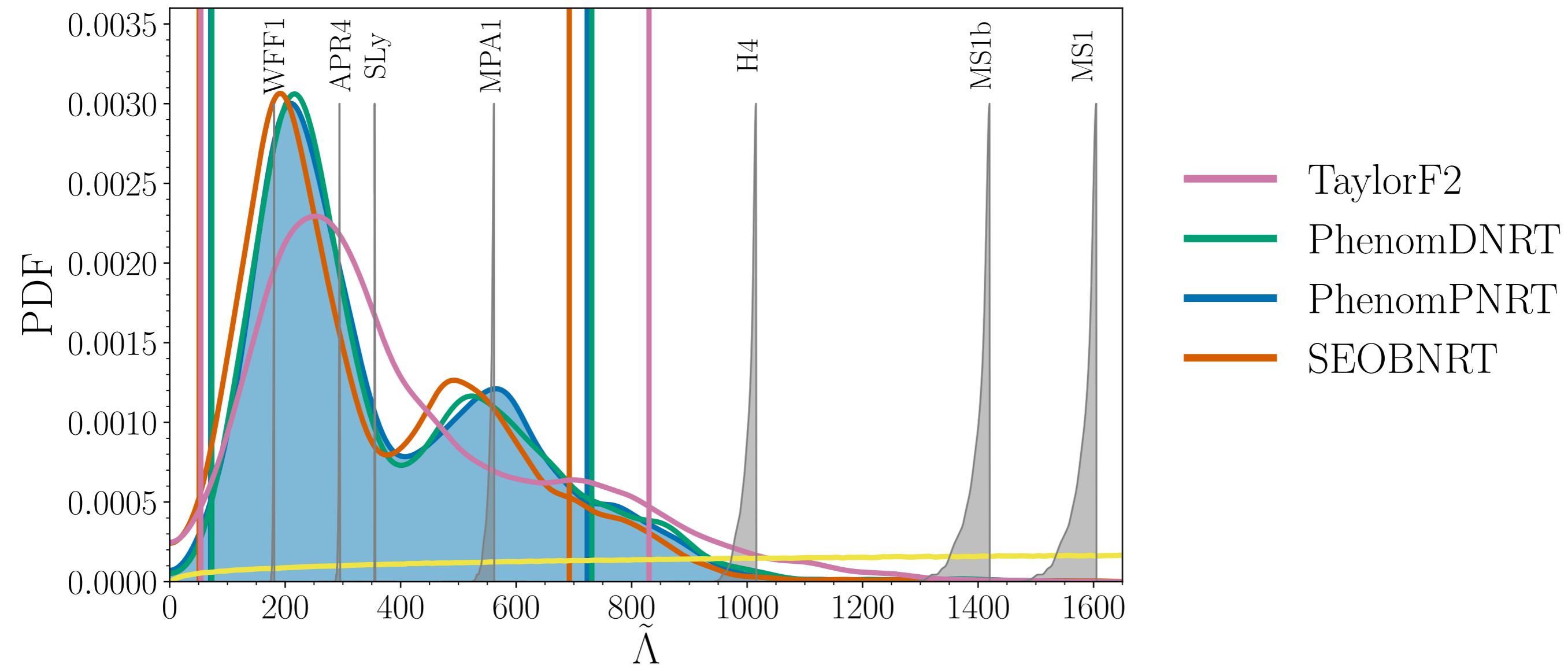
$$\tilde{\Lambda} = 222.29^{+419.83}_{-138.48} \quad 245.39^{+453.12}_{-151.53} \quad 233.39^{+447.55}_{-144.40}$$



Mass prior	$\tilde{\Lambda}$	\hat{R} (km)
Uniform	310^{+679}_{-234}	$11.3^{+2.4}_{-2.4} \pm 0.2$
Double neutron star	354^{+691}_{-245}	$11.6^{+2.3}_{-2.1} \pm 0.2$
Galactic neutron star	334^{+669}_{-241}	$11.5^{+2.3}_{-2.2} \pm 0.2$

Improved analysis of GW170817

[LVC,1805.11579]



Using sophisticated waveform models (**NRTidal**), an updated highest-posterior-density (HPD) interval,

$$\tilde{\Lambda} = 300^{+420}_{-230}$$

If a common EOS is assumed, this is further

restricted to $\tilde{\Lambda} = 190^{+390}_{-120}$

Parameter estimation methods
A. Data and Bayesian inference

Our independent reanalysis of GW170817

- **NR calibrated tidal waveform models**
- flat prior on $\tilde{\Lambda}$, $\tilde{\Lambda} \sim U[0, 3000]$

basically following those adopted in the improved LVC analysis
(e.g., arXiv:1805.11579)

or our previous study (TN+, Phys. Rev. Res. 2019).

- Bayesian inference, Nested sampling implemented in LALInference.
- The sky position is fixed to the location determined by optical followup observations.
- BayesLine PSD

Bayesian parameter estimation of GWs

Why Bayesian statistics and stochastic sampling

- A lot of parameters
- Parameter estimation (PE)
- Model selection

Bayes' theorem

$$L(d|\vec{\theta}) \propto \exp\left(-2 \int_0^\infty \frac{|\tilde{d}(f) - h(\vec{\theta}, f)|^2}{S_n(f)} df\right)$$

Prior

Likelihood

Posterior

$$p(\vec{\theta}|\{d\}, H) = \frac{p(\vec{\theta}|H)p(\{d\}|\vec{\theta}, H)}{P(\{d\}|H)}$$

Evidence for the model H $P(\{d\}|H) \equiv Z_H$

H: hypothesis (signal embedded in data), {d}: data set, θ : parameters

- $23 \text{ Hz} \leq f \leq f_{\text{max}}$, $f_{\text{max}} = 1000 \text{ Hz}$ or 2048 Hz ($\min[f_{\text{isco}}, f_s/2]$), $f_s = 4096 \text{ Hz}$.

We calculate posterior with Nested sampling
(LIGO Algorithm Library (LAL), LALInference)

Parameter estimation methods

B. *Waveform models for inspiraling BNSs*

The gravitational waveform $\tilde{h}(f) = A(f)e^{i\Psi(f)}$

where the amplitude and the phase

$$A(f) = A_{\text{point-particle}}(f) + A_{\text{spin}}(f) + A_{\text{tidal}}(f)$$

$$\Psi(f) = \Psi_{\text{point-particle}}(f) + \Psi_{\text{spin}}(f) + \Psi_{\text{tidal}}(f)$$

BBH baseline: PP + Spin

- TF2
- TF2+

Tidal contribution

- **KyotoTidal**
- NRTidal
- NRTidalv2
- PNTidal

Model name Point-particle part

Amplitude Phase

TF2 3PN 3.5PN

TF2+ **6PN** **6PN**

Model name Tidal part

Amplitude Phase

KyotoTidal Polynomial Nonlinear

NRTidal - Pade approx.

NRTidalv2 Pade approx. Pade approx.

PNTidal 5+1PN 5+2.5PN

BBH baseline: PP + Spin

- TF2
- **TF2+**

Model	Point-particle part	
	Amplitude	Phase
TF2	3PN	3.5PN
TF2+	6PN	6PN

TaylorF2 waveform (TF2) [Blanchet+2006, Buonanno+2009]

with point-particle phase up to 3.5PN-order + spin

$$\Psi_{\text{point-particle}}(f) = 2\pi f t_c - \phi_c - \frac{\pi}{4} + \frac{3}{128\eta} x^{-5/2} \left\{ 1 + \left(\frac{3715}{756} + \frac{55}{9}\eta \right) x - 16\pi x^{3/2} + \dots \right\}$$

$$\eta = m_1 m_2 / (m_1 + m_2)^2$$

0PN

1PN

1.5PN

where the dimensionless post-Newtonian (PN) parameter

$$x = (\pi M_{\text{tot}} f)^{2/3}$$

The best estimated mass parameter is the chirp mass

$$\mathcal{M} = \frac{(m_1 m_2)^{3/5}}{(m_1 + m_2)^{1/5}} \simeq \frac{c^3}{G} \left[\frac{5}{96} \pi^{-8/3} f^{-11/3} \dot{f} \right]^{3/5}$$

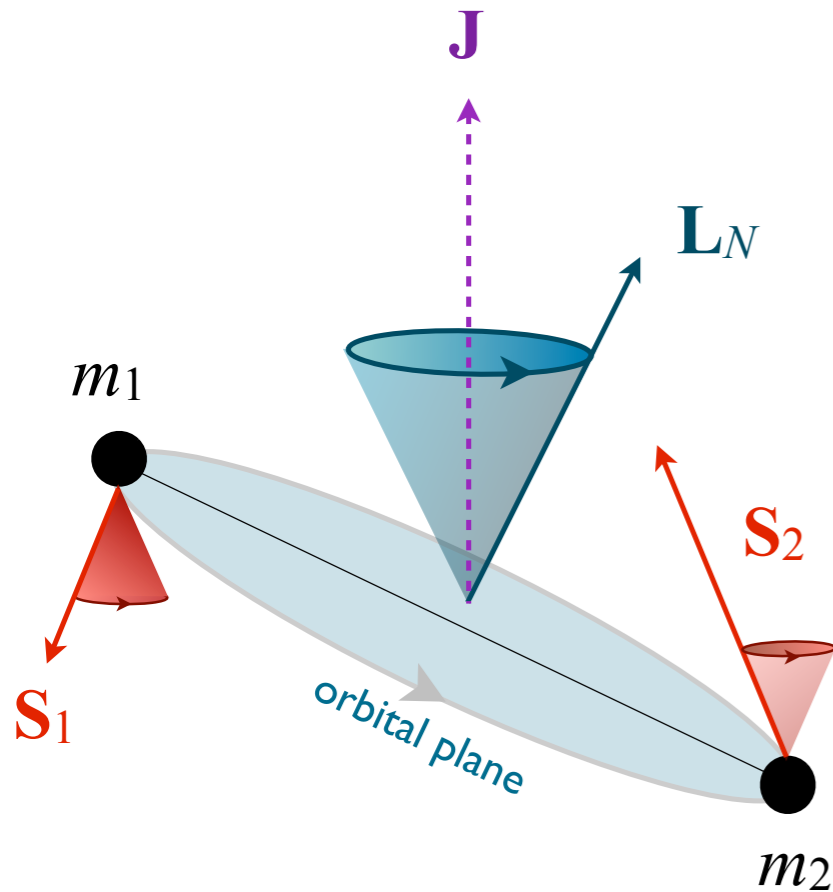
and only place weak constraints on the mass ratio $q = m_2/m_1 \leq 1$ and the spin.

TF2+ adds high-PN order terms to TF2.

[Kawaguchi+, 2018]

Spin contribution

$$\mathbf{J} = \mathbf{L} + \mathbf{S}_1 + \mathbf{S}_2$$



If $\mathbf{S}_{1,2}$ misaligned with respect to \mathbf{L} , they cause the binary's orbital plane to precess around the almost-constant direction of the total angular momentum of the binary, \mathbf{J} .

We assume that the spins are aligned with \mathbf{L} .

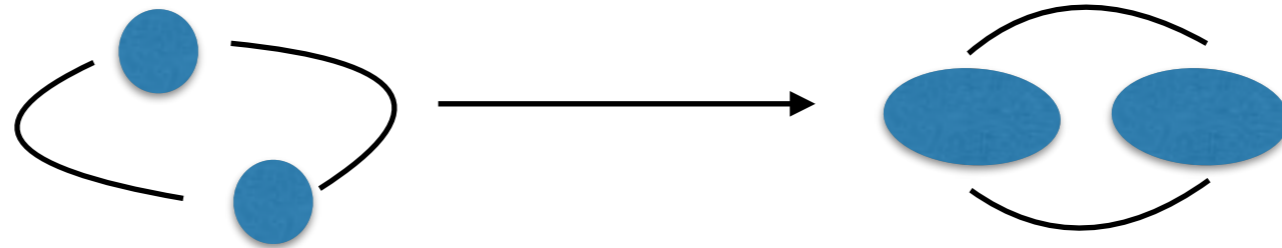
dimensionless spin magnitude $\chi = c |\mathbf{S}| / (Gm^2) \leq 1$

a simple mass-weighted linear combination of the spins

$$\chi_{\text{eff}} = \frac{c}{G} \left(\frac{\mathbf{S}_1}{m_1} + \frac{\mathbf{S}_2}{m_2} \right) \cdot \frac{\hat{\mathbf{L}}}{M},$$

which takes values between -1 (both objects have maximal spins antialigned with respect to \mathbf{L}) and $+1$ (maximal aligned spins).

Tidal effects



When binary orbital separations are small, each star is tidally distorted by its companion.

tidal deformability: $\lambda = -\frac{Q: \text{(tidal induced) quadrupole moment}}{\varepsilon: \text{companion's tidal field}}$

The information about the NS EOS can be quantified by λ .

The leading order tidal contribution to GW phase

[Vines, Flanagan & Hinderer 2011]

$$\Psi_{\text{tidal}} = \frac{3}{128\eta} \left[-\frac{39}{2} \tilde{\Lambda} x^{5/2} \left(1 + \frac{3115}{1248} x \right) \right]$$

5PN 5+1PN

binary tidal deformability, mass-weighted combination of $\Lambda_{1,2}$

$$\tilde{\Lambda} = \frac{16}{13} \frac{(m_1 + 12m_2)m_1^4\Lambda_1 + (m_2 + 12m_1)m_2^4\Lambda_2}{(m_1 + m_2)^5}$$

$\Lambda = \lambda/m^5$: dimensionless

PNTidal
 (Post-Newtonian)
 5+2.5PN

$$\Psi_{\text{tidal}}^{\text{PNTidal}} = \frac{3}{128\eta} \left[-\frac{39}{2} \tilde{\Lambda} x^{5/2} \right. \\
\left. \times \left(1 + \frac{3115}{1248} x - \pi x^{3/2} + \frac{28024205}{3302208} x^2 - \frac{4283}{1092} \pi x^{5/2} \right) \right]$$

5PN
5+1PN
5+1.5PN
5+2PN
5+2.5PN

5+1PN [Vines, Flanagan & Hinderer, (2011)]

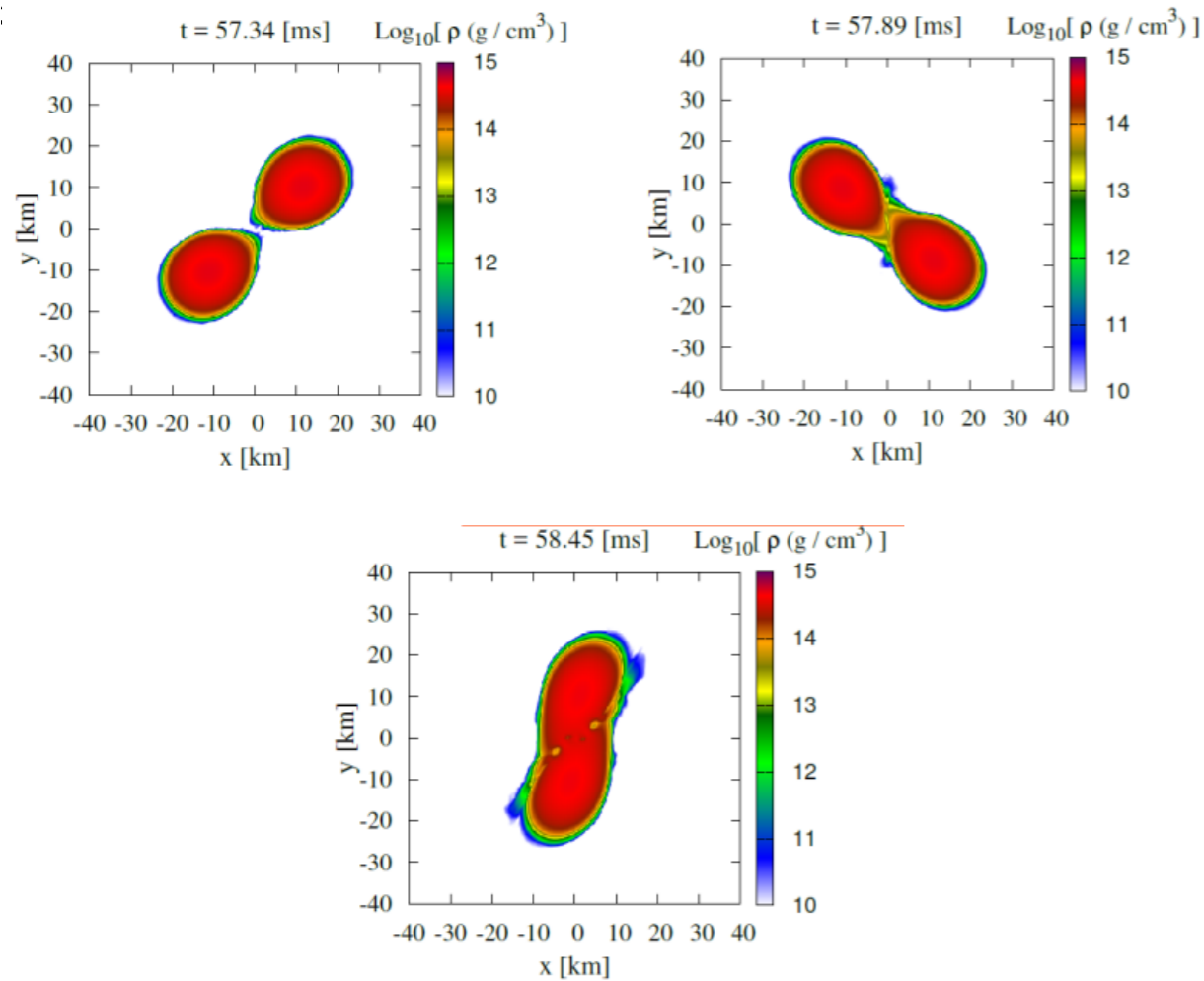
5+2.5PN [Damour, Nagar & Villain, (2012)]

$$A_{\text{tidal}}^{\text{PNTidal}} = \sqrt{\frac{5\pi\eta}{24}} \frac{M_{\text{tot}}^2}{d_L} \tilde{\Lambda} x^{-7/4} \\
\times \left(-\frac{27}{16} x^5 - \frac{449}{64} x^6 \right)$$

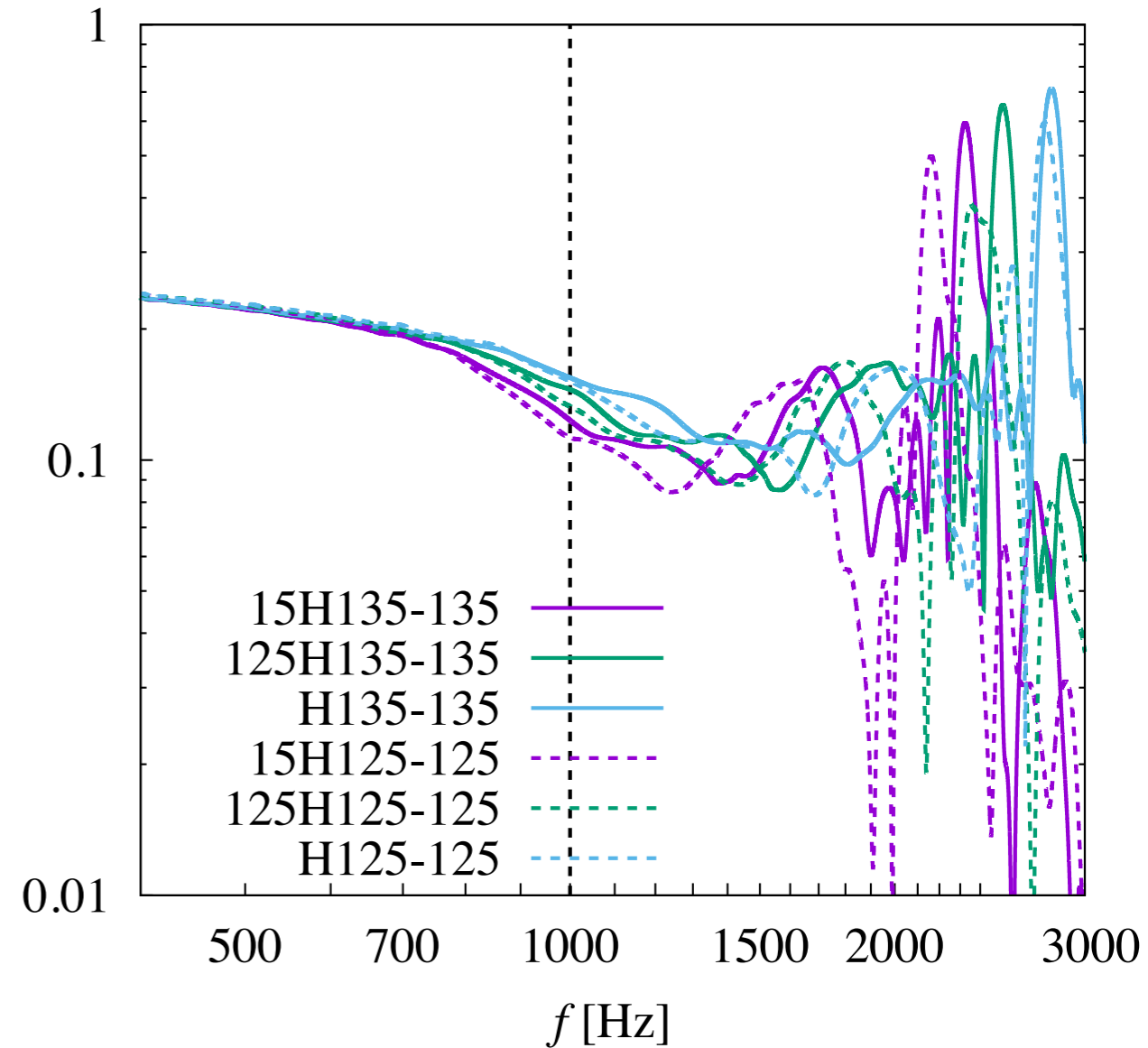
5PN 5+1PN

Numerical Relativity calibrated waveforms for inspiraling BNS

Kiuchi+, "Sub-radian-accuracy gravitational waveforms of coalescing BNSs in NR", 2017.



$f A D_{\text{eff}} / m_0$



NR calibrated waveform model, **TF2+_KyotoTidal**

point-particle: **TF2+**, calibrated by SEOBNRv2

tidal: **KyotoTidal**, calibrated by hybrid waveform (SEOBNRv2T+NR)

Kawaguchi+, 2018

KyotoTidal

(NR calibrated)

[Kawaguchi, et al., 2018]

Nonlinear
correction

$$\Psi_{\text{tidal}}^{\text{KyotoTidal}} = \frac{3}{128\eta} \left[-\frac{39}{2} \tilde{\Lambda} \left(1 + a \tilde{\Lambda}^{2/3} x^p \right) \right] x^{5/2}$$
$$\times \left(1 + \frac{3115}{1248} x - \pi x^{3/2} + \frac{28024205}{3302208} x^2 - \frac{4283}{1092} \pi x^{5/2} \right)$$

5PN 5+1PN 5+1.5PN 5+2PN 5+2.5PN

$$A_{\text{tidal}} = \sqrt{\frac{5\pi\eta}{24}} \frac{m_0^2}{D_{\text{eff}}} \tilde{\Lambda} x^{-7/4}$$
$$\times \left(-\frac{27}{16} x^5 - \frac{449}{64} x^6 - 4251 x^{7.890} \right).$$

5PN

5+1PN

higher-order tidal effects

NRTidal

(NR calibrated)

$$\Psi_{\text{tidal}}^{\text{NRTidal}} = \frac{3}{128\eta} \left[-\frac{39}{2} \tilde{\Lambda} x^{5/2} \right. \\ \left. \times \frac{1 + \tilde{n}_1 x + \tilde{n}_{3/2} x^{3/2} + \tilde{n}_2 x^2 + \tilde{n}_{5/2} x^{5/2}}{1 + \tilde{d}_1 x + \tilde{d}_{3/2} x^{3/2}} \right]$$

[Dietrich, et al., 2017]

Pade approx. (Linear)

NRTidalv2

(NR calibrated)

$$\Psi_{\text{tidal}}^{\text{NRTidalv2}} = \frac{3}{128\eta} \left[-\frac{39}{2} \tilde{\Lambda} x^{5/2} \right. \\ \left. \times \frac{1 + \tilde{n}'_1 x + \tilde{n}'_{3/2} x^{3/2} + \tilde{n}'_2 x^2 + \tilde{n}'_{5/2} x^{5/2} + \tilde{n}'_3 x^3}{1 + \tilde{d}'_1 x + \tilde{d}'_{3/2} x^{3/2} + \tilde{d}'_2 x^2} \right]$$

[Dietrich, et al., 2019]

Pade approx. (Linear)

$$A_{\text{tidal}}^{\text{NRTidalv2}} = \sqrt{\frac{5\pi\eta}{24}} \frac{M_{\text{tot}}^2}{d_L} \tilde{\Lambda} x^{-7/4} \\ \times \left(-\frac{27}{16} x^5 \right) \frac{1 + \frac{449}{108} x + \frac{22672}{9} x^{2.89}}{1 + dx^4}$$

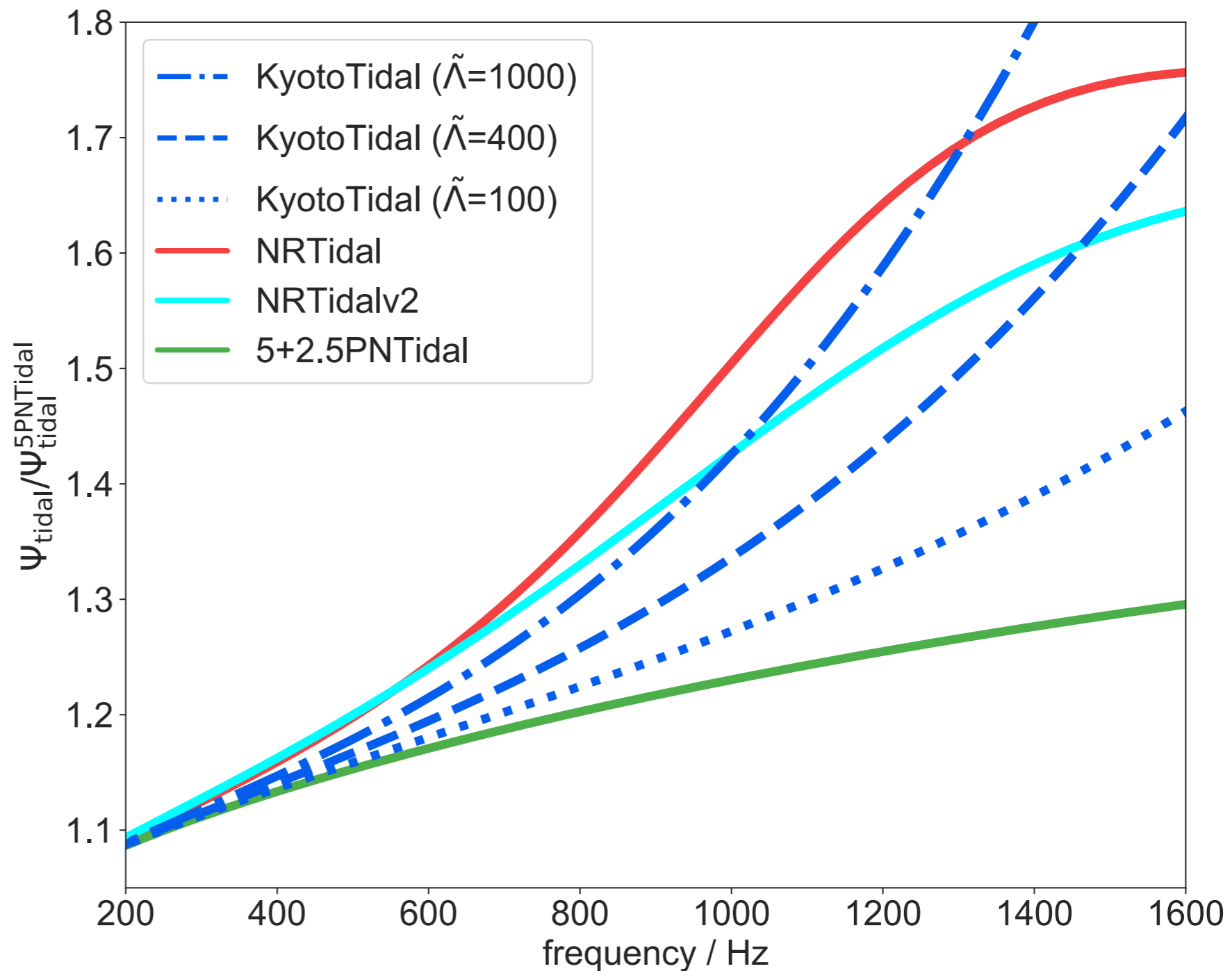
Pade approx. (Linear)

Tidal waveform models

divided by the leading tidal formula.

phase shift:

1. NRTidal
2. NRTidalv2
3. KyotoTidal (Lamtilde=400)
4. PNTidal



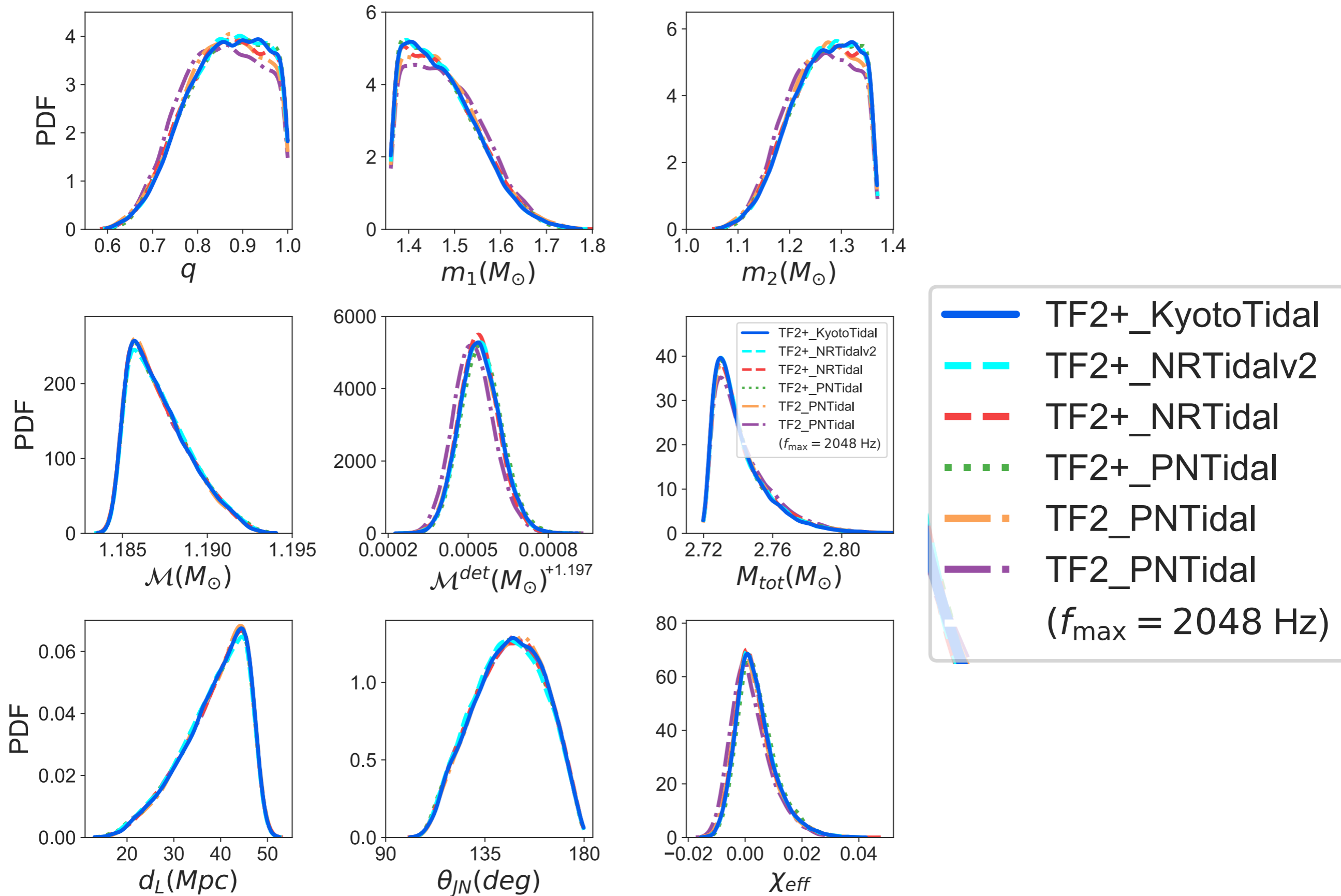
Model name	Point-particle part		Tidal part	
	Amplitude	Phase	Amplitude	Phase
TF2_PNTidal	3PN	3.5PN	5+1PN	5+2.5PN
TF2+_PNTidal	6PN	6PN	5+1PN	5+2.5PN
TF2+_KyotoTidal	6PN	6PN	Polynomial	Non-linear
TF2+_NRTidal	6PN	6PN	-	Padé approximation
TF2+_NRTidalv2	6PN	6PN	Padé approximation	Padé approximation

Source parameters

- parameters for BNS $\{m_{1,2}, \chi_{1,2}, \tilde{\Lambda}\}$
 - $m_{1,2} \sim U[0.83, 7.7]M_{\odot}$, $M_c^{\text{det}} \sim U[1.184, 2.168]M_{\odot}$
 - $\chi_{1,2} \sim U[-0.05, 0.05]$
 - $\tilde{\Lambda} \sim U[0, 3000]$
- additional parameters for fully describe the binary:
 $\{D_L, \theta_{JN}, \psi, t_c, \phi_c, \alpha, \delta\}$
 - a uniform prior in $[0, 2\pi]$ for ϕ_c .
 - sources uniformly distributed in volume

Results

A. Source properties other than the tidal deformability



Almost no systematic bias associated with a difference in the estimates of the parameters among waveform models.

Results

B. Posterior of binary tidal deformability

Comparison with LIGO-Virgo analysis as a sanity check

restricted TF2 with 5+1 PN-order tidal phase

uniform prior on $\Lambda_{1,2}$

$f_{\max}=2048$ Hz

HPD

Symmetric interval (Highest probability distribution)

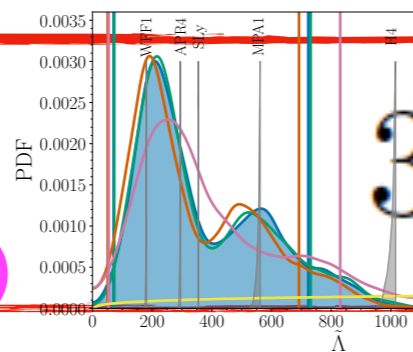
HLV
(our results)

347^{+564}_{-243}

347^{+453}_{-295}

very close!

HLV
(LVC report,
arXiv:1805.11579)



340^{+580}_{-240}

(340^{+490}_{-290})

HLV

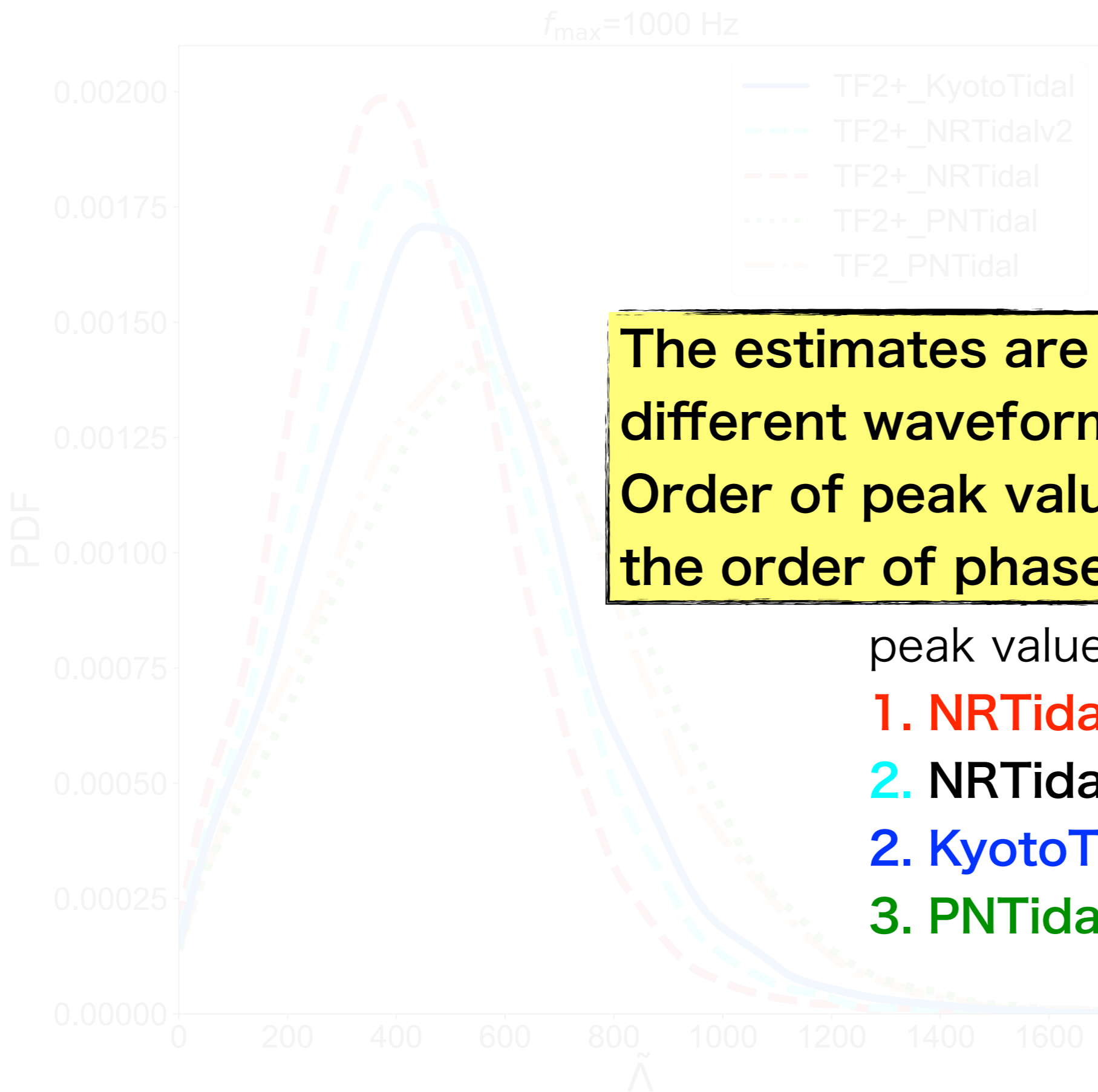
(our results,

flat prior on Λ_{tilde})

316^{+504}_{-224}

(316^{+367}_{-291})

Posterior of binary tidal deformability



likely ~400,
not above 1000

The estimates are biased by using different waveform models. Order of peak value is consistent with the order of phase shift.

peak value:

1. **NRTidal**

2. **NRTidalv2**

2. **KyotoTidal**

3. **PNTidal**

phase shift:

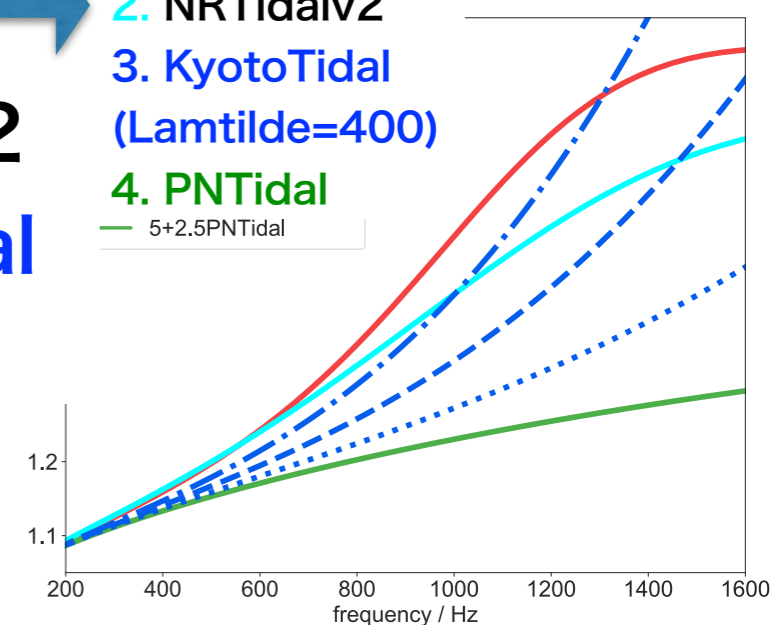
1. **NRTidal**

2. **NRTidalv2**

3. **KyotoTidal**
($\tilde{\Lambda}=400$)

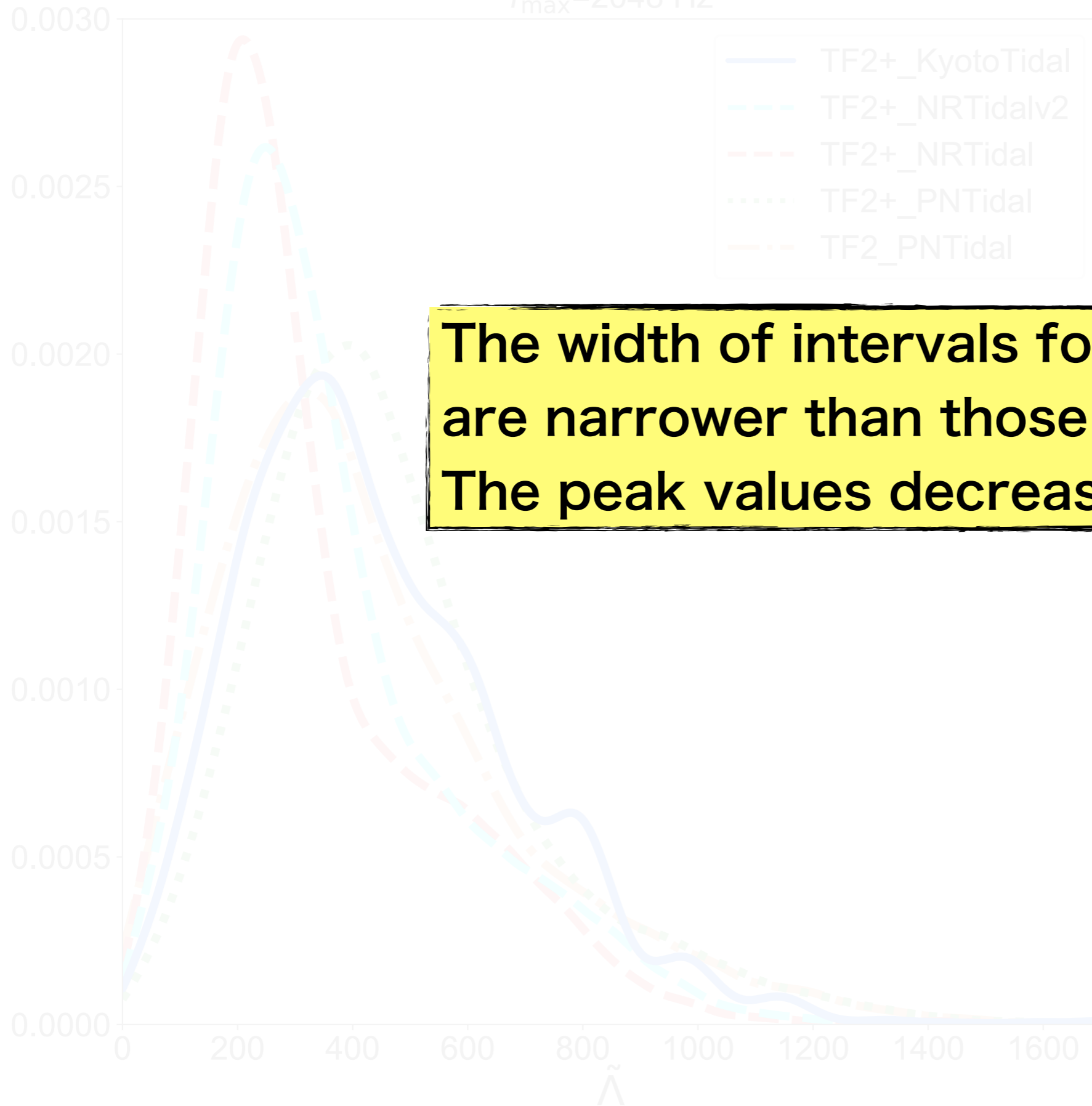
4. **PNTidal**

5. **5+2.5PNTidal**



For $f_{\max}=2048$ Hz (only a reference)

$f_{\max}=2048$ Hz



The width of intervals for $f_{\max}=2048$ Hz are narrower than those for $f_{\max}=1000$ Hz. The peak values decrease as f_{\max} increases.

peak value:

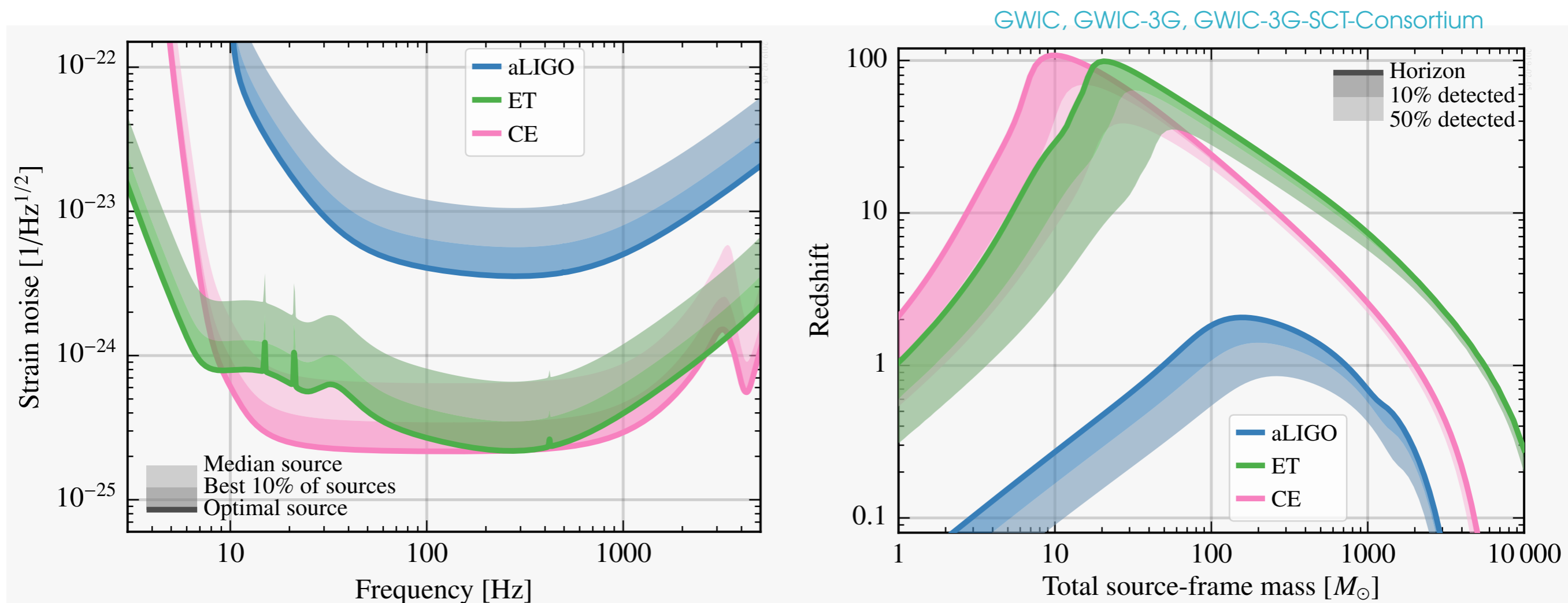
1. NRTidal
2. NRTidalv2
2. KyotoTidal
3. PNTidal

Discussion

need to improve the current waveform model

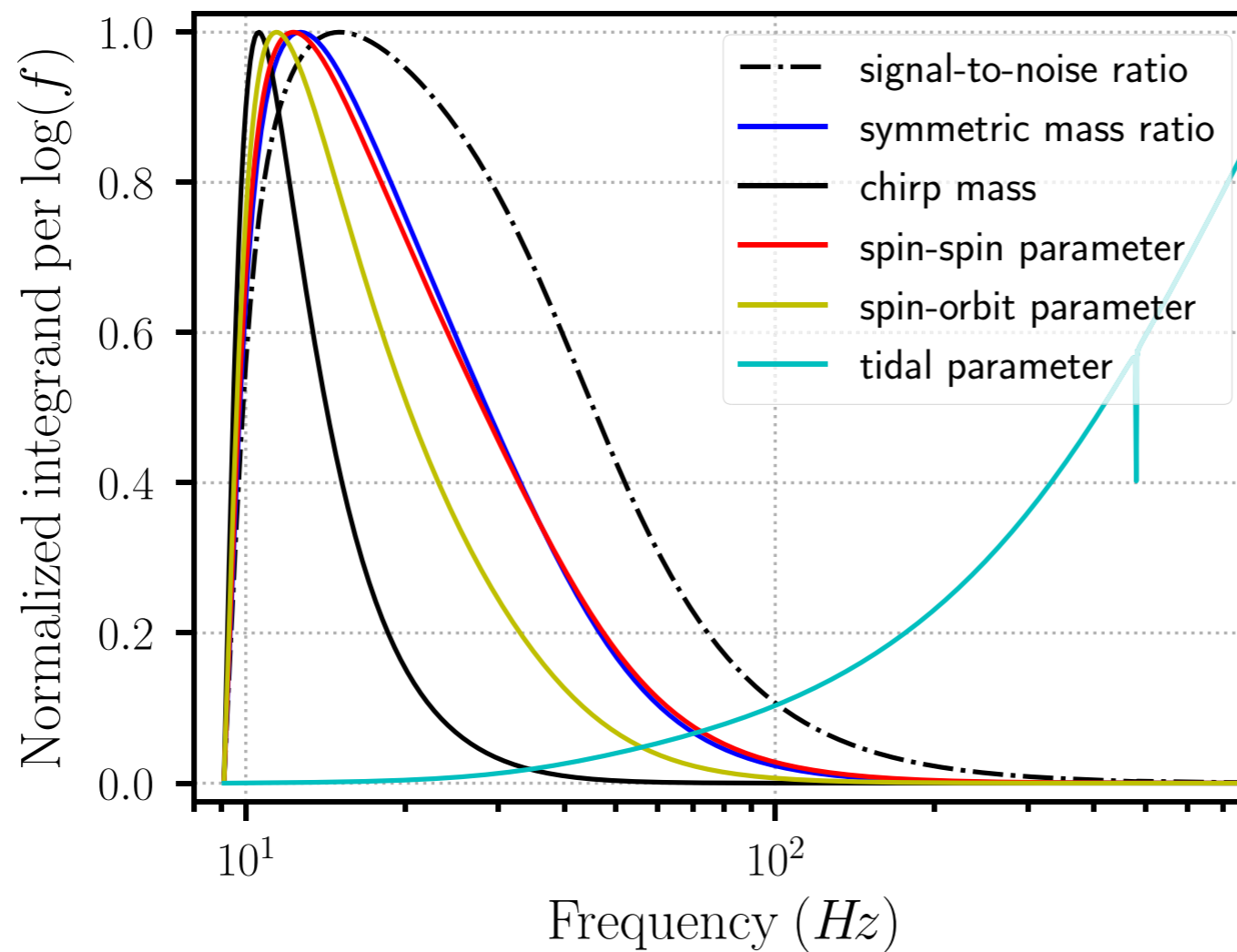
Systematic error for $f_{\max}=1000$ Hz

For GW170817, systematic error is dominant over statistical error. For 10 times louder SNR event than GW170817, systematic error between KyotoTidal and NRTidal is comparable with the statistical error. 3G detector's sensitivity is 10 times better than current detectors. Toward 3G detector era, it is needed to improve current waveform models.



Need to improve at frequency higher than 1000 Hz

High frequency data are generally more informative to measure tidal deformability. Our results indicate that $\tilde{\Lambda}$ is indeed constrained tighter determined for $f_{\max}=2048$ Hz than for $f_{\max}=1000$ Hz. However, since the TF2+ KyotoTidal model is calibrated by NR waveforms only up to 1000 Hz, toward 3G detector era, it is needed to further improve the model in the frequency higher than 1000 Hz.



[Harry, Hinderer, 2018]
(c.f. [Damour, Nagar, Villain, 2012])

Summary

- LIGO-Virgo Collaboration put conservative upper limits on tidal deformability with post-Newtonian waveform (**PNTidal**) and measure it with **NRTidal**.
- We reanalyze GW170817 with a new NR calibrated waveform model, **KyotoTidal**.
- We compare our results with another NR calibrated waveform, **NRTidal** and its upgraded model, **NRTidalv2**.

The estimates are biased by using different waveform models. Order of peak value is consistent with the order of phase shift.

The width of intervals for $f_{\max}=2048$ Hz are narrower than those for $f_{\max}=1000$ Hz. The peak values decrease as f_{\max} increases.